RESEARCH ARTICLE OPEN ACCESS

Mechanical Behavior of Asphaltic Mixtures Produced with Spray Graphite in High Energy Mill

Alex Gomes Pereira*, Juliano Rodrigues Spínola*, Anne Karollynne Castro Monteiro*, Benício de Morais Lacerda**, Fábio dos Santos Gusmão*, Consuelo Alves da Frota*

**(Geotechnical Research Group, Federal University of Amazonas, Brazil*
***(Professor at Porto Velho School of Education and Culture, UNESC, Brazil)*
Corresponding Author: Alex Gomes Pereira

ABSTRACT
The work evaluates the mechanical behavior of two types of asphalt concrete, one representing the conventional mixture and the other identifying the alternative composition with high energy mill pulverized graphite. Complex modulus and phase angle were determined in prismatic specimens using the Pneumatic 4 Point Bending Apparatus. The methodology employed uniaxial sinusoidal compression loading, strain amplitude of 50 μm/m; frequencies of 0.1 Hz, 0.2 Hz, 0.5 Hz, 1 Hz, 2 Hz, 5 Hz, 10 Hz and 20 Hz and temperatures from 0 °C to 40 °C in increments of 5 °C. The results showed that the composition with the participation of the ground graphite in 4 hours time presented higher values of complex modulus and phase angle relative to conventional asphalt concrete.

Keywords **-** Four-point bending, complex modulus, phase angle, graphite, asphalt concrete.

Date Of Submission: 06-11-2019 Date Of Acceptance: 26-11-2019

I. INTRODUCTION

Road pavements are a multilayer system with different materials, which are subjected to stress resulting from numerous loading combinations from traffic and environmental conditions (KIM, 2009). When they are flexible, they have an upper layer, whose participant, petroleum asphalt cement, binds mineral materials, coarse aggregates, fine aggregates and filler (HAFEEZ et al. 2012).

One way to verify the performance of these compositions in terms of viscoelastic behavior is to determine the stress-strain behavior defined by the complex modulus (E*) and phase angle (δ). Such parameters can be obtained through tests according to bar flexion, uniaxial compression in cylindrical samples, mechanical wave propagation (CLYNE et al. 2003), or through prediction models based on aggregate particle size and asphalt binder characteristics (WITCZACK & FONSECA, 1996).

In the case of the four-point bending test, the prismatic specimens are subjected to sinusoidal load pulses in the middle thirds of the prismatic specimens. The test is performed at different frequencies, which may vary from 0.1 Hz to 50 Hz, and various temperatures, from -30 °C to 40 °C, by means of recommendations as prescribed by EN 12697-24. According to Colpo (2014), when sinusoidal loads are transmitted, there is the same level of displacement to the lower and upper side, with constant and alternating displacement amplitudes over time.

In determining the complex modulus, one-dimensional sinusoidal loading and the resulting voltage can be represented by Equations 1 and 2, respectively (KIM, 2009). Figure 1 schematically presents such features. Thus, the complex modulus E * can be defined by the relationship between sine stress and strain (Equation 3).

$$\sigma^* = \sigma_0 e^{i\omega t} \quad (1)$$

$$\varepsilon^* = \varepsilon_0 e^{i(\omega t - \varphi)} \quad (2)$$

$$\frac{\sigma^*}{\varepsilon^*} = E^*(i\omega) = \left(\frac{\sigma_0}{\varepsilon_0}\right) e^{i\varphi} = E_1 + E_2 \quad (3)$$

Where σ0 corresponds to the stress amplitude, ε0 the strain amplitude, t the time, φ the phase angle, which is the time difference between the stress and strain peaks, and ω the angular velocity, associated with the frequency (Equation 4). It is noteworthy that E1 and E2 represent, respectively, the real part (storage modulus or elastic) and the imaginary part (viscous modulus).

$$\omega = 2\pi f \quad (4)$$

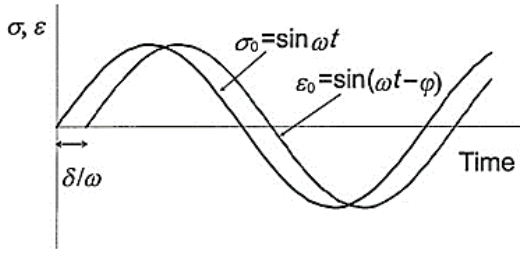

Figure 1: Schematic sinusoidal loading
Source: Kim (2009).

The relationship between stress amplitude and strain (Equation 5) is defined as the dynamic module |E*|, given by the absolute value of the complex module E*. Figure 2 shows the complex plane, where the real and imaginary parts of the complex module are described by Equation 6.

$$\left|E^*(\omega)\right| = \sqrt{E_1^2 + E_2^2} = \frac{\sigma_0}{\varepsilon_0} \tag{5}$$

$$E^* = E_1 + E_2 \tag{6}$$

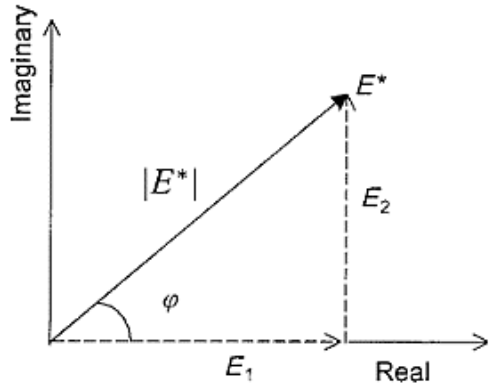

Figure 2: Schematic representation of the complex module in the complex plane
Source: Kim (2009).

It is also emphasized that the modules E1 and E2 can be represented as a function of the phase angle according to Equations 7 and 8. Centofante (2016) explains that the phase angle can be described as an indicator of viscous properties material and conceived as the delay angle of ε0 relative to σ0 (Equation 9).

$$E_1 = \frac{\sigma_0 \cos\varphi}{\varepsilon_0} \tag{7}$$

$$E_2 = \frac{\sigma_0 \sin\varphi}{\varepsilon_0} \tag{8}$$

$$\delta = \frac{t_i}{t_p} x360 \tag{9}$$

Here ti represents the fraction of time between stress and strain peaks, tp the time of a charge cycle and ω is the angular frequency.

In this scenario, we study the mechanical behavior of conventional asphalt concrete (CA-REF) and high-energy mill pulverized asphalt concrete (CA-GRAFM) according to different loading temperatures and frequencies. For example, the determination of the complex modulus and phase angle under four-point flexion.

II. MATERIALS AND METHODS

The following materials were part of the surveyed asphalt compositions: coarse aggregate, gravel 1 (Figure 3 (a)) and gravel 0 (Figure 3 (b)); fine aggregate, sand (Figures 3 (c)) and stone dust (Figure 3 (d)); two fillers, Portland cement composing the reference mixture (CA-REF) and graphite ground for 4 hours forming the alternative mixture (CA-GRAFM); and petroleum asphalt cement, CAP 50/70 (Figure 3 (e)).

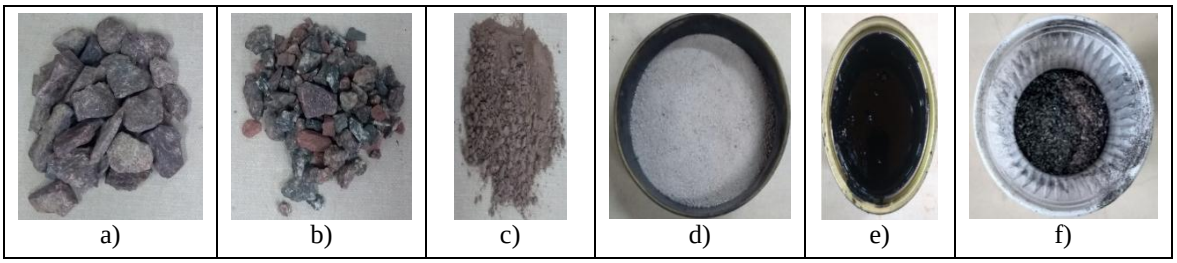

Figure 3: a) gravel 1; b) gravel 0; c) dust; d) sand; e) petroleum asphalt cement; f) graphite.

The natural graphite shown in Figure 3 (f) was sprayed into a high energy mill (MAE) for 15, 30, 60 and 240 min. As a rule, the reduction in grain size leads to an increase in the specific surface of the material, which therefore enhances its properties (JACKSON & SHERMAN, 1953; DAS, 2014). The graphite grinding methodology followed the following steps: a) Weighing with a precision of ± 0.001 g; b) Inserting the material into a cylindrical jar (D = 2 ¼ ”and h = 3”) with a load capacity of up to 10 g, together with two ½ inch steel balls to then start the mechanical amorphizing process. Figures 4 (a) and 4 (b) illustrate the physical appearance of the samples before and after the milling process for 240 minutes, respectively.

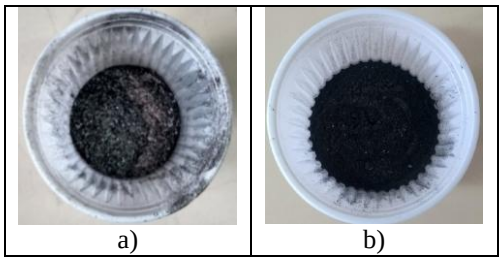

a) b)

Figure 4: Graphite: a) before the process; b) after grinding process.

Aggregates were analyzed by the parameters Gsa (Apparent Specific Gravity), Gsb (Bulk Specific Gravity), absorption, hardness and particle size according to the methodologies of the American Society for Testing and Materials (ASTM). As for the characterization of the properties of the 50/70 asphalt binder, they followed the specifications of the National Agency of Petroleum, Natural Gas and Biofuels (ANP), which uses ASTM methods. Density-ground graphite was examined based on ASTM C188/17 - Standard Test Method for Density of Hydraulic Cement and crystalline structure by x-ray diffractometry. In this experiment, we used the Empyrean PANalytical equipment, with Cu-Kα radiation (λ=0.1541838 nm), according to an angular range of 5-120º of 2θ, and a rate of 0.02º/min.

The reference dosage was one used by the City Hall of Manaus, capital of the State of Amazonas, in the construction of paved roads, which consists of 14.30% of gravel 1, 28.40% of gravel 0, 25.40% stone dust, 23.70% sand, 3% Portland cement and 5.20% asphalt binder.

The beam compaction process was conducted by means of a hydraulic press with a maximum capacity of 30 tons. These specimens were subjected to the four-point bending test, the experimental apparatus which are shown in Figures 5 (a) and 5 (b). The adopted methodology followed the recommendations of the European standard EN 12697-26, with application of sinusoidal load and strain amplitude of 50 μm/m. The load application frequency series followed the values of 0.1, 0.2, 0.5, 1, 2, 5, 10, 20 Hz; and the recommended temperatures followed the range of 0 ° C to 40 °C, with increments of 5 in 5 °C. For each temperature, the minimum acclimatization time established by EN 12697-26 was adopted.

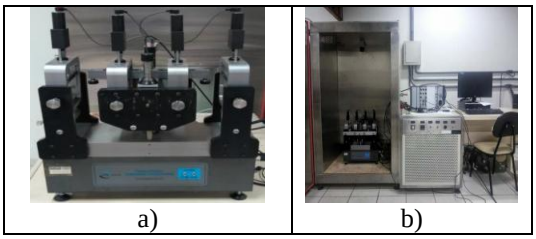

a) b)

Figure 5: a) 4-point test apparatus; b) climate camera.

III. RESULTS AND DISCUSSIONS

Table 1 presents the values obtained from the characterization assays. It is noteworthy in these results that the absorption of gravel 1 and 0 showed low values, that is, less than 2 %; as well as the value of the Los Angeles abrasion, which is below the 50 % limit set by the National Department of Transportation Infrastructure (DNIT ME - 035/98).

The particle size characteristics of the materials are shown in Figure 6 and Table 2. By analyzing the particle size and uniformity and curvature coefficients together, and according to the Unified Soil Classification System, they are classified as: poorly graded gravel, gravel 1 and 0; poorly graded sand, residual sand; and well-graded sand, stone dust. Portland cement and graphite are fully meshed to No. 200 mesh (0.075 mm), therefore meeting the requirements for use as filler (ASTM C117/17 - Standard Test Method for Materials Finer than 75-μm (No. 200) Sieve in Mineral Aggregates by Washing).

Table 1: Characterization of aggregates.

Properties	Result
Apparent specific gravity (Gsa) of the coarse aggregate - Gravel 1	2.58 g/cm³
Bulk specific gravity (Gsb) of the coarse aggregate - Gravel 1	2.55 g/cm³
Absorption of coarse aggregate - Gravel 1	0.51 %
Apparent specific gravity (Gsa) of the coarse aggregate - Gravel 0	2.74 g/cm³
Bulk specific gravity (Gsb) of the coarse aggregate - Gravel 0	2.62 g/cm³
Absorption of coarse aggregate - Gravel 0	1.66 %
Apparent specific gravity (Gsa) of aggregate fine – sand	2.21 g/cm³
Apparent specific gravity of cement - Portland cement	2.94 g/cm³
Apparent specific gravity (Gsa) of aggregate fine - dust	2.75 g/cm³
Hardness (Los Angeles abrasion) - Gravel 1	14.10 %
Hardness (Los Angeles abrasion) - Gravel 0	27.39 %
Apparent specific gravity of cement – Graphite	2.64 g/cm³

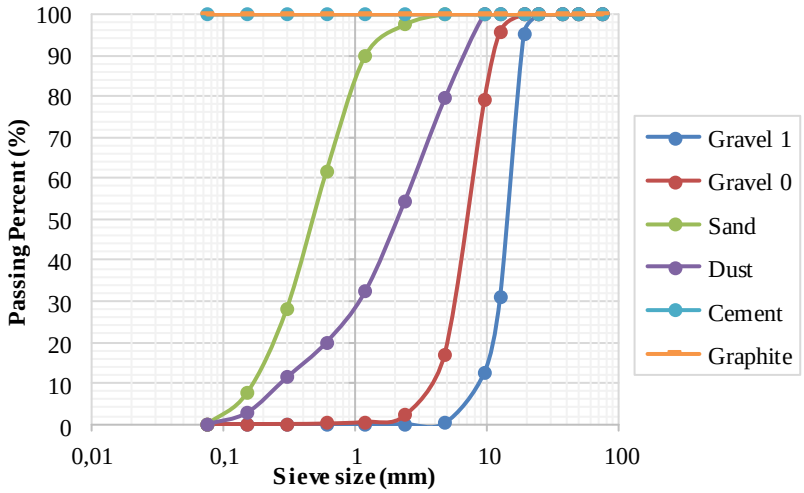

Figure 6: Material particle size curves.

Table 2: Aggregate Uniformity and Curvature Coefficients.

Materials	Cu	Cc
Gravel 1	1.81	1.16
Gravel 0	1.91	0.97
Sand	3.38	1.06
Dust	11.49	1.58

Table 3 presents the values of the asphalt cement characterization tests. Through this table, it is verified that Penetration classified petroleum asphalt cement as 50/70; The Softening Point and Flash Point have met the specifications, ie they are above the minimum value established by standard; The values for Saybolt Furol and Brookfield viscosities at temperatures 135, 150 and 177 °C were within the specified limits; Solubility in trichlorethylene and ductility showed satisfactory results; and the parameters after the aging process of the samples, in rotary thin-film oven (RTFOT), also met the recommendations of ASTM.

Table 3: Asphalt Binder Properties.

Features	Unity	Oil Asphalt Cement		Methods
		Result	Limits	ASTM
Penetration -5s, 25 °C	0,1 mm	69	50-70	D5
Softening Point, min	°C	49.7	>46	D 36
Saybolt Furol Viscosity at 135 °C	s	283	>141	E 102
Saybolt Furol Viscosity at 150 °C	s	140.7	>50	E 102
Saybolt Furol Viscosity at 177 ° C	s	50.8	30-150	E 102
Brookfield Viscosity at 135 °C	cP	539	>274	D 4402
Brookfield Viscosity at 150 °C	cP	279.8	>112	D 4402
Brookfield Viscosity at 177 ° C	cP	96.8	57-285	D 4402
Flash point, min	°C	318	>235	D 92
Solubility in Trichloroethylene	%	99.5	>99.5	D 2042
RTFOT Bulk Variation	%	0.04	<0.5	D 2872
Ductility at 25 °C	cm	> 100	60	D 113
RTFOT softening point increase	°C	7.1	<8	D 36
RTFOT retained penetration	%	63	>55	D 5

Figure 7 illustrates representative diffractograms of the natural and sprayed graphite samples for the 15, 30, 60 and 240 minute times. It is noted from Figure 7 (a) that the peaks of post milled materials exhibited reduced intensity and flares relative to natural graphite. As shown in Figure 7 (b), which illustrates the second peak of the diffractograms, it appears that the graphite sprayed for 240 minutes (4h) exhibited a differentiated enlargement compared to the other samples, pointing to the formation of a new crystal structure and reduction of the average particle size. This new arrangement may be related to the shear process and the impact of the spheres on the particles (CARREÑO, 2008). According to Jackson & Sherman (1953) and Das (2014), the reduction of particle size promotes the increase of a specific surface area and, consequently, increases its

cohesive power in a composition. Thus, based on these results, we chose to use graphite subjected to a high energy mechanical grinding for 4 h.

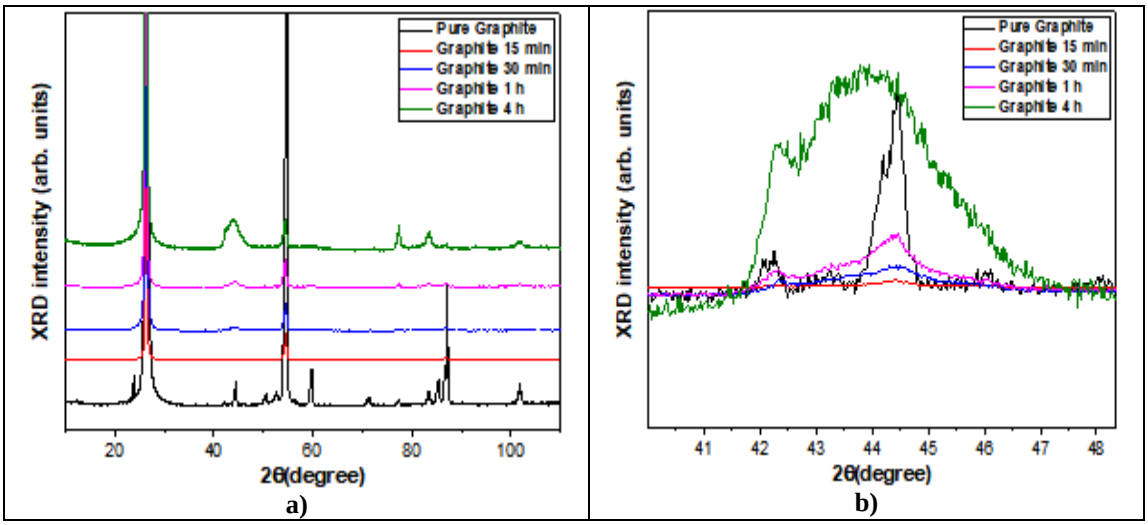

Figure 7: a) diffractogram of natural graphite samples; b) diffractogram of graphite samples, second peak.

In order to systematically show the kinetic susceptibility of the compositions, the isothermal curves presented in Figure 8 were elaborated, which correlate the complex modules (ordered) as a function of the loading frequencies (abscissa) at different temperatures. An increase in the complex modulus can be observed for the asphalt mixture produced with pulverized graphite, an expected trend in the research in question, from the mechanical amorphization of the natural graphite.

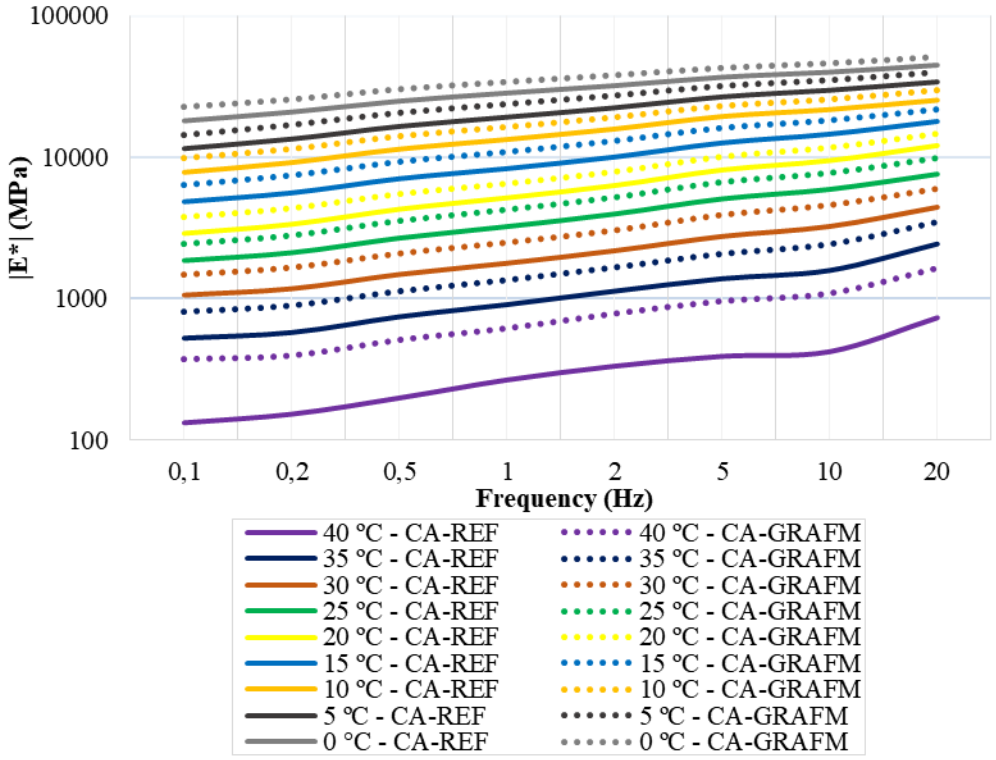

Figure 8: Comparison of isothermal curves for the studied asphalt mixtures.

In order to improve understanding, two isothermal curves (Figure 9) were selected from Figure 8, corresponding to the temperature of 25 ºC and 40 ºC, which is representative of the Manaus (AM/BR) asphalt pavement surface. In these curves, it is verified that the behavior of asphalt concretes,

from the inclination of the isotherms, demonstrates an increase in stiffness, as the loading frequency increases. In particular, this increasing inclination characterizes the vertical displacement of alternative compositions relative to conventional formulation. It is also observed that the lower the temperature, the greater the stiffness gains from the incorporation of alternative materials. In addition, it was observed that sensitivity increases with temperature, an indicated behavior for all mixtures.

In general, this behavior is considered an important characteristic of asphalt concrete, because gains in this respect portray less damage to the permanent deformation of the asphalt mixture, under stresses from various load combinations. In short, the addition of sprayed graphite material increased the pavement life due to better response to permanent deformations. Such response was also observed in the works of Melo (2014), Melo and Trichês (2016), Marcon (2016) and Carlesso (2017), Carlesso et al. (2019), who adopted the same study methodology, although the experiments were performed with modified binders and with different compaction processes.

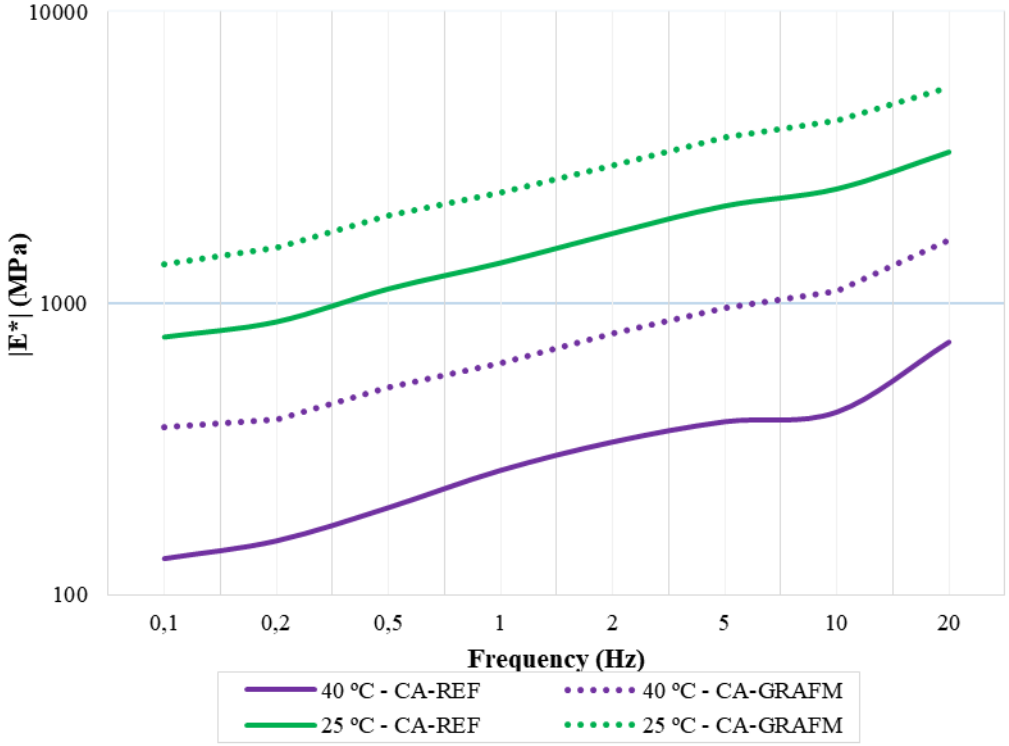

Figure 9: Isothermal curves, temperatures 25 ºC and 40 ºC.

Examining also the mechanical behavior, there is Table 4 which shows, in percentage terms, the increase of stiffness, ie, it explains the gains of the complex module of the alternative formulation CA-GRAFM relative to the CA-REF mixture. Also according to these results for the CA-GRAFM composition, and taking the frequency of 10 Hz as an example, representing a speed around 72 km/h (CHABOT et al., 2011), the increase of the complex modulus, relative to the standard mixture, is on the order of 57.84 %, 29.23 %, 23.20 % and 23.11 %, for temperatures of 30 ºC, 25 ºC, 20 ºC and 15 ºC, respectively. It is emphasized that, in practice, increased stiffness portrays a higher angular coefficient in the stress-strain curve. This indicates that the stiffness of the CA-GRAFM mixture in the field, under the same stress state subjected to standard formulation, would be less sensitive to tensile deformations in the bottom fiber of the asphalt coating layer.

Table 4: Variation of the complex module for pulverized graphite asphalt Mix compared to conventional asphalt mix (in percentage Terms).

T (ºC)	0	5	10	15	20	25	30
f (Hz)	CA-GRAFM						
0.1	23.65	61.89	37.26	48.34	102.44	50.97	61.01
0.2	19.92	61.21	27.56	53.68	84.74	48.90	66.32
0.5	23.44	56.76	20.80	46.41	65.32	43.35	64.27
1	20.73	47.88	17.03	44.11	49.02	35.55	61.62
2	24.84	40.99	11.52	38.22	40.23	28.83	58.96
5	22.40	26.52	2.55	33.21	29.16	31.10	64.04
10	26.16	16.76	1.95	23.11	23.20	29.23	57.84
20	26.93	18.51	5.91	10.98	8.38	33.35	53.83

In order to portray the elastic behavior of asphalt mixtures, and to avoid possible discrepancies in the experimental results (AIREY, 2002), Figure 10 shows the Black diagrams for the CA-REF and CA-GRAFM mixtures, which relate the complex modulus (scale logarithmic values) with the respective phase angle values (arithmetic scale) as a function of the loading frequency and test temperature. According to the said figure, there is a shortening of the Black space of the sprayed graphite mixture compared to the reference composition. In addition, a tendency to increase phase angles is observed as the test temperature is increased. Therefore, the incorporation of the alternative material, in general, generates a reduction of the phase angles, making the samples more elastic.

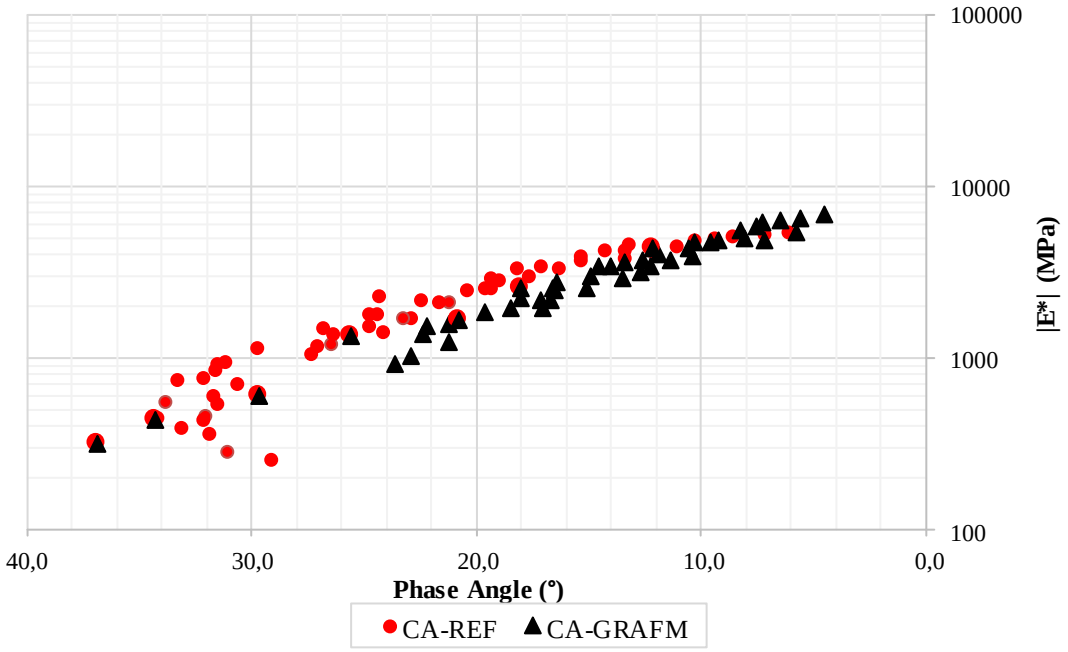

Figure 10: Comparison of Black Spaces, CA-REF Mix vs. CA-GRAFM Mix

It is noteworthy that no corresponding studies were found in the specialized literature on the replacement of traditional filler (Portland cement) with alternative materials, in particular the use of ground graphite in the studied asphalt concrete formulation (CA-GRAFM) under flexural flexure four points. The works cited (MELO, 2014; MELO & TRICHÊS, 2016; MARCON, 2016; CARLESSO, 2017; AND CARLESSO et al. 2019), although they performed a similar experiment, researched compositions with the participation of modified binders and compaction using the compactor table. LCPC, those are very different conditions of the present study.

IV. CONCLUSION

The main purpose of this research was to determine the mechanical behavior of asphaltic concretes produced with 4 h sprayed graphite, relative to the reference composition, as well as to obtain the viscoelastic properties. Considering the analyzes performed in relation to the conventional formulation, it was observed that the addition of

ground graphite in the asphalt mixtures showed a higher kinetic behavior, associated with an increase in the complex modulus for all the studied temperatures; and by the Black diagrams, the reduction of the phase angles was verified, showing the plasticity increase with the presence of this alternative material, that is, the CA-GRAFM asphalt concrete presented higher resistance to permanent deformation.

From the above, the results showed satisfactory performance of asphalt mixtures produced with pulverized graphite, compared to the conventional formulation. This conclusion contributes to ratify the use of this alternative material in asphalt compositions as an alternative to the traditional filler (Portland cement).

ACKNOWLEDGEMENTS

The authors thank the Construction and Paving Company LTDA (ARDO) for donating the materials used in this research, as well as the Coordination for the Improvement of Higher Education Personnel (CAPES) for the scholarship grant. The authors also thank the Materials Laboratory (LabMat/UFAM) for their support in carrying out chemical and diffraction tests and the Geotechnical Research Group (GEOTEC/UFAM) where all the physical and mechanical experiments were performed.

REFERENCES

[1]. AIREY, G.D. (2002). Use of black diagrams to identify inconsistencies in rheological data. Road Materials and Pavement Design, 3(4), 403-424.

[2]. ASTM - American Society for Testing Materials. ASTM C117: Standard Test Method for Materials Finer than 75-µm (No. 200) Sieve in Mineral Aggregates by Washing. USA, 2017.

[3]. _____. ASTM C 127: Standard test method for density, relative density (specific gravity), and absorption of coarse aggregate. USA, 2015.

[4]. _____. ASTM C 128: Standard Test Method for Relative Density (Specific Gravity) and Absorption of Fine Aggregate. USA, 2015.

[5]. _____. ASTM C 131: Standard Test Method for Resistance to Degradation of Small-Size Coarse Aggregate by Abrasion and Impact in the Los Angeles Machine. USA, 2014.

[6]. _____. ASTM C 136: Standard Test Method for Sieve Analysis of Fine and Coarse Aggregates. USA, 2006.

[7]. _____. ASTM C 188: Standard Test Method for Density of Hydraulic Cement. USA, 2017.

[8]. _____. ASTM D 5: Standard test method for penetration of bituminous materials. USA. 2013.

[9]. _____. ASTM D 36: Standard test method for softening point of bitumen (ring-and-ball apparatus). USA. 2014.

[10]. _____. ASTM D 4402: Standard test method for viscosity determination of asphalt at elevated temperatures using a rotational viscometer. USA. 2013.

[11]. _____. ASTM D 92: Standard Test Method for Flash and Fire Points by Cleveland Open Cup Tester. USA, 2018.

[12]. _____. ASTM D 113: Standard Test Method for Ductility of Asphalt Materials. USA, 2017.

[13]. _____. ASTM D 2042: Standard Test Method for Solubility of Asphalt Materials in Trichloroethylene. USA, 2015.

[14]. _____. ASTM D 2872: Standard Test Method for Effect of Heat and Air on a Moving Film of Asphalt (Rolling Thin-Film Oven Test). USA, 2012.

[15]. _____. ASTM E 102: Standard Test Method for Saybolt Furol Viscosity of Bituminous Materials at High Temperatures. USA, 2016.

[16]. CARLESSO, G. C. Estudo do comportamento de mistura asfáltica modificada por nanoargila e polímero SBS. Dissertação (mestrado) - Universidade Federal de Santa Catarina. Centro Tecnológico. Programa de Pós-Graduação em Engenharia Civil. Florianópolis, 2017.

[17]. CARLESSO, G. C.; TRICHÊS, G.; De Melo, J. V.S.; MARCON, M. F.; THIVES, L. P.; DA LUZ, L. C. Evaluation of Rheological Behavior, Resistance to Permanent Deformation, and Resistance to Fatigue of Asphalt Mixtures Modified with Nanoclay and SBS Polymer. Applied Sciences-Basel, v. 9, p. 2697-2713, 2019.

[18]. CARRENO, N. L. V.; GARCIA, I. T. S.; LEITE, E. R.; SANTOS, L. P. S.; KEYSON, D.; LONGO, E.; FAJARDO, H. V.; PROBST, L. F. D.; FABBRO, M. T. Nanocompósitos cerâmicos a partir do processo de moagem mecânica de alta energia. Química Nova, v. 31, p. 962-968, 2008.

[19]. CENTOFANTE, R. Estudo laboratorial da utilização de material fresado em misturas asfálticas recicladas a quente. Dissertação (mestrado) - Universidade Federal de Santa Maria. Centro de Tecnologia. Programa de Pós-Graduação em Engenharia Civil. Santa Maria, RS, 2016.

[20]. CHABOT, A.; CHUPIN, O.; DELOFFRE, L.; DUHAMEL, D. Viscoroute 2.0: A tool for

simulation of moving load effects on asphalt pavement. Journal Road Materials and Pavement Design. 2011, 11, 227–250.
[21]. CLYNE T. R.; MIHAI X. L.; MARASTEANU O.; EUGENE L., Dynamic and Resilient Modulus of Mn/Dot Asphalt Mixtures, Technical Report, MN/RC 2003-09, Department of Civil Engineering, University of Minnesota, Minneapolis, USA (2003).
[22]. COLPO, G. B. Análise de fadiga de misturas asfálticas através do ensaio de flexão em viga quatro pontos. 2014. 154p. Dissertação (Mestrado em Geotecnia) - Universidade Federal do Rio Grande do Sul, 2014.
[23]. DAS, B.M. Fundamentos de engenharia geotécnica. Cengage Learning, 2015.
[24]. DEPARTAMENTO NACIONAL DE INFRAESTRUTURA DE TRANSPORTES (DNIT). ME 035:1998: Agregados - determinação da abrasão "Los Angeles". Rio de Janeiro, 1998.
[25]. EN - European Standard. EN 12697-26: Bituminous mixtures - test methods for hot mix asphalt, part 26: Stiffness. CEN, Brussels. 2004.
[26]. HAFEEZ, I., KAMAL, M. A., AHADI, M. R., SHAHZAD, Q., BASHIR, N., Performance Prediction of Hot Mix Asphalt from Asphalt Binders, Pakistan Journal of Engineering and Applied Sciences, 2012, 104-113.
[27]. LOULIZI, A.; FLINTSCH, G. W.; AL-QADI, I. L.; MOKAREM, D. Comparison between Resilient Modulus and Dynamic Modulus of Hot-Mix Asphalt as Material Properties for Flexible Pavement Design, Transportation Research Record Journal of the Transportation Research Board, 2006, 161-170.
[28]. JACKSON, M. L.; SHERMAN, G. D. Chemical weathering of minerals in soil. Adv. Agron, 1953, 211-318.
[29]. KIM, Y. R. Modeling of asphalt concrete. United State of America: ASCE Press, 2009.
[30]. MARCON, M. F. Estudo e comparação do desempenho mecânico e reológico entre concretos asfálticos modificados por polímero SBS, borracha moída de pneu e nanomateriais. Dissertação (Mestrado) – Programa de Pós-Graduação em Engenharia Civil, Universidade Federal de Santa Catarina, Florianópolis, 2016.
[31]. MELO, J. V. S. Desenvolvimento e estudo do comportamento reológico e desempenho mecânico de concretos asfálticos modificados com nanocompósitos. Tese de Doutorado - Programa de Pós-Graduação em Engenharia Civil, Universidade Federal de Santa Catarina, Florianópolis, 2014.
[32]. MELO, J. V. S.; TRICHÊS, G. Evaluation of properties and fatigue life estimation of asphalt mixture modified by organophilic nanoclay. Construction and Building Materials, v. 140, p.
[33]. 364-373, 2017.
[34]. WITCZAK, M. W.; FONSECA, O. A., Revised Predictive Model for Dynamic (Complex) Modulus of Asphalt Mixtures, Transportation Research Record, 1996, 15-23.

Alex Gomes Pereira "Mechanical Behavior of Asphaltic Mixtures Produced with Spray Graphite in High Energy Mill" International Journal of Engineering Research and Applications (IJERA), vol. 9, no. 11, 2019, pp 18-26